ACS APPLIED MATERIALS & INTERFACES

Research Article

www.acsami.org

Nanodiamond Promotes Surfactant-Mediated Triglyceride Removal from a Hydrophobic Surface at or below Room Temperature

Xianjin Cui,[†] Xianping Liu,[‡] Andrew S. Tatton,[§] Steven P. Brown,[§] Haitao Ye,[⊥] and Andrew Marsh*[,†]

[⊥]School of Engineering and Applied Science, Aston University, Birmingham, B4 7ET United Kingdom

[†]Department of Chemistry, [‡]School of Engineering, and [§]Department of Physics, University of Warwick, Coventry, CV4 7AL United Kingdom

Supporting Information

ABSTRACT: We demonstrate that ca. 5 nm nanodiamond particles dramatically improve triglyceride lipid removal from a hydrophobic surface at room temperature using either anionic or nonionic surfactants. We prepare nanodiamond–surfactant colloids, measure their stability by dynamic light scattering and use quartz crystal microbalance–dissipation, a technique sensitive to surface mass, in order to compare their ability to remove surface–bound model triglyceride lipid with ionic and nonionic aqueous surfactants at 15–25 °C. Oxidized, reduced, ω-alkylcarboxylic acid, and ω-alkylamidoamine surface-modified adducts are prepared, and then characterized by techniques including ^{13}C cross-polarization (CP) magic-angle spinning (MAS) NMR. Clear improvement in removal of triglyceride was observed in the presence of nanodiamond, even at 15 °C, both with nanodiamond–surfactant colloids, and by prior nanoparticle deposition on interfacial lipid, showing that nanodiamonds are playing a crucial role in the enhancement of the detergency process, providing unique leads in the development of new approaches to low-temperature cleaning.

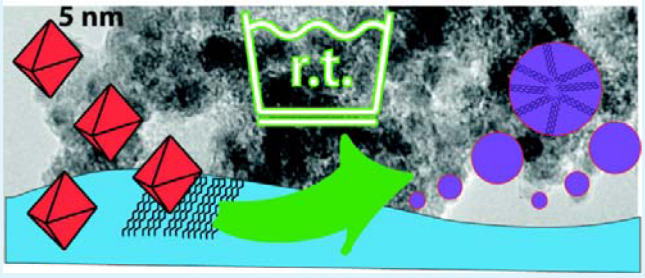

KEYWORDS: *nanodiamond, tristearin, lipid removal, detergency, surfactant, zeta potential, quartz crystal microbalance (QCM), QCM with dissipation monitoring (QCM-D)*

INTRODUCTION

The removal of complex crystallized lipid in laundry soil, ("sebum": usually modeled by a triglyceride such as tristearin), is time- and energy-intensive requiring high temperature, even with modern detergents.[1−6] The UK consumer performs an average of five washes at 90 °C and 83 at 60 °C each year, at up to 2.7 and 1.6 kWh per wash, respectively, in order to remove this soil.[7] The major cost is in heating water, hence consumer and industry desire for low-temperature cleaning where energy consumption might be reduced to 0.1−0.2 kWh for 20 °C wash cycles. Methods typically used for cleaning include mechanical abrasion, enzymes[8] to break down polymeric protein soils and hydrolyze triglycerides,[5,9] together with surfactants at higher temperature.[10−13] Although enzymes are key ingredients in modern detergents, those currently available are ineffective at hydrolyzing crystallized lipid at room temperature, requiring both effective adsorption and high mobility on the lipid surface to facilitate the key catalytic activity at the water–lipid interface.[9,14] Glucose-derived nonionic surfactants including decyl β-D-glucopyranoside,[15−18] or surfactant mixtures[19] have been found to be more efficient than many amphiphiles at removing tristearin from model surfaces.[15,16] Optimum detergency of nonionic surfactants, including these, occurs above the phase inversion temperature, which can be reduced by adding a small amount of lipophilic amphiphile,[1,20,21] or by making the surfactants more hydrophobic. This approach has also been explored to enhance cleaning at lower temperatures,[19,22] although the effects of nanoparticulates have not been studied. We speculated that detonation diamond nanoparticles ('nanodiamond'),[23,24] known to possess hydrophobic features, may aid the removal of lipid from surfaces at room temperature, plausibly by aiding the detergency of surfactants, in addition to altering the lipid surface upon deposition, and other mechanisms. Nanodiamonds possess a surprisingly large surface area that can adsorb lipid and/or other small molecules,[25,26] and offer opportunities for further functionalization[27] in order to tune surface properties. Nanoparticles' (or carbon nanotubes')[28] tendency to self-aggregate in air and aqueous solution, in order to minimize surface energy brings a barrier to their use, usually mitigated by surface modification[29−31] or surfactant additives[32−34] that stabilize colloidal nanoparticle suspensions. In this work, we initially explored a range of anionic (sodium dodecylbenzenesulfonate, SDBS), nonionic (decyl β-D-glucopyranoside, G_1C_{10}; decyl β-D-maltopyranoside, G_2C_{10}; polyoxyethylene(12) nonylphenyl ether, NFE_{10}; and polyethyleneglycol dodecyl ether, Brij35) and zwitterionic (*N*,*N*-dimethyldodecylamine *N*-oxide, DDAO) surfactants with untreated nanodiamonds. We then also

Received: March 30, 2012
Accepted: June 6, 2012
Published: June 7, 2012

Table 1. Lipid Removal by Anionic Surfactant SDBS with and without Prior Deposition of Nanoparticles, T = 25 °C[a]

entry	nano- diamond	[SDBS] (mmol L^{-1})	zeta potential (mV)	t (min)	R_1 (Hz)	R_2 (Hz)
1	none present	1	n.d.	n.d.	−30	No removal
2	ND97	1	ca. 15[c]	5	−300	10
3	none present	20	n.d.	7	−30	19
4	ND97	20	ca. 15[c]	20	−220	60
5	none present	40	n.d.	2	350 ± 90	520 ± 30
6	ND97	40	ca. 15[c]	120	650 ± 110	860 ± 140
7	**3**	40	26.1	110[b]	580 ± 125	730 ± 80[b]
8	**2**	40	41.5	170	540 ± 40	670 ± 70
9	**4**	40	48.1	600[b]	370	590[b]
10	**2** and **1**	40	<41.5	65	300	570
11	**4** and **1**	40	<48.1	204	660 ± 10	940 ± 160

[a]For meaning of R_1 and R_2, please refer to main text. Compound key: **1** = oxidized nanodiamond, **2** = hydrogenated nanodiamond, **3** = *ω-tert*-amine functionalized nanodiamond, **4** = *ω*-carboxylic acid functionalized nanodiamond. Error bars represent standard deviation of duplicate measurements. t is the time taken to reach equilibrium. n.d. = value not determined. [b]The system did not reach equilibrium. [c]Approximate value because the colloid was unstable over time.

modified the nanoparticles' surface chemistry to further understand mechanisms for the effects we observed, using ^{13}C cross-polarization (CP) magic-angle spinning (MAS) nuclear magnetic resonance NMR to confirm structure. Dynamic light scattering (DLS) was applied to characterize the stability of nanodiamond colloids or suspensions, and quartz crystal microbalance with dissipation monitoring (QCM-D)[35−38] used in order to study the lipid removal process.[11,15]

EXPERIMENTAL SECTION

Tristearin lipid and cetyltrimethylammonium bromide (CTAB) were purchased from Tokyo Chemical Industry (TCI) Ltd. Diamond nanopowder 97% (ND97) and all other reagents were purchased from Sigma-Aldrich and used without further purification. Zeta potential of particles in solution were measured by dynamic light scattering (DLS) on a Malvern Zetasizer at 25 °C, in Milli-Q water with a neutral pH value from 7.0 to 7.2. QCM data were recorded on a Q-Sense E4 from *Q-Sense AB*, Sweden at a 25 °C and processed using Q-Tools software.[9,37,39] Raman spectra were recorded on a Renishaw inVia Raman Microscope with a CCD detector and a laser of 514.5 nm. Infrared (IR) Spectra were recorded on a PerkinElmer Spectrum 100 FT-IR spectrometer, using attenuated total reflectance. Scanning Electron Microscopy (SEM) images were obtained on JEOL 4500 FIB/SEM, and thermogravimetric analysis (TGA) was carried out on a Mettler Toledo DSC1−400 under N_2 with a heating rate of 10 °C/minute. ^{13}C CP MAS experiments were recorded using a Bruker Avance II+ spectrometer operating at a ^1H Larmor frequency of 599.4 MHz (B_0 = 14.1 T). Experiments described in panels a and c in Figure 6 were recorded using a Bruker 3.2 mm HX probe, whereas the experiment in (b) was recorded using a Bruker 2.5 mm triple resonance probe, operating in double resonance mode. An MAS frequency of 20 kHz was used for all spectra presented. A ^1H pulse of duration 2.5 μs was used to excite initial transverse magnetization. The number of coadded transients recorded for each spectrum was (a) 14436, (b) 10980 and (c) 2000, with recycle delays of (a) 3 s, (b) 2 s, and (c) 3 s. ^{13}C magnetization was created using a cross-polarization ramp[40] of magnitude 80% to 100%, with a contact time of duration (a) 3 ms, (b) 2 ms, and (c) 3 ms. SPINAL-64[41] heteronuclear decoupling was applied during acquisition at a ^1H nutation frequency of 100 kHz, for (a) 10 ms, (b) 12 ms, and (c) 10 ms. All resonances are referenced to the carboxylic acid group in L-alanine at 177.8 ppm, which corresponds to a primary reference to tetramethylsilane (TMS) at 0 ppm.

Preparation of 1. Commercial ND97 was heated in air in a tube furnace at over 400 °C for 1−5 h, with a heating rate of 10 °C/minute.

Preparation of 2. Commercial ND97 was treated with hydrogen plasma in a custom-made molybdenum container within an ASTeX 5010 (Seki Technotron Corp., 2.45 GHz, 1.5 kW) MPCVD system. Hydrogen plasma was achieved by heating the 200 S.C.C.M (standard cubic centimeter per minute) diluted hydrogen flow under pressure of 50 Torr. The ND97 powder was kept in the resultant plasma for 10 min and then cooled in H_2 atmosphere.

Preparation of *ω*-Alkylcarboxyl-Functionalized Diamond Nanoparticles 3,. *Route A.* A suspension of **2** (100 mg) in toluene (50 mL) was sonicated for 1 h; 10-undecenoic acid (3 mL) was then added and the resultant mixture sonicated for a further hour. The reaction was then irradiated with UV light (254 nm) for 6 h with vigorous stirring. The product **3** was collected by centrifugation as a powder, washed with ethanol 5 times, and dried at 60 °C under vacuum.

Route B. A suspension of **2** (100 mg) in triethylamine (50 mL) was sonicated for 1 h then 10-undecenoic acid (3 mL) was added dropwise. The resultant mixture was sonicated for a further hour, then irradiated with UV light (254 nm) for 6 h with vigorous stirring. The product **3** was obtained as a solid by centrifugation and washed with ethanol, 3 M HCl and water.

Preparation of *ω*-Alkylamine-Functionalized Diamond Nanoparticles 4. This was carried out in toluene using the same method as for **3**, with 1-(4-methylpiperazin-1-yl)undec-10-en-1-one in place of 10-undecenoic acid.

Preparation of QCM Sensor and Lipid Removal Experiments. All QCM sensors used in this paper are gold coated quartz crystals from Q-Sense, with a fundamental frequency of 5 MHz. The gold QCM sensor exhibited a water contact angle of 62° and in order to obtain a hydrophobic surface suitable for tristearin deposition, sensors were coated with a self-assembled octadecylmercaptan ($CH_3(CH_2)_{17}SH$) monolayer as follows. Crystals were immersed in $CHCl_3$ for 12 h to remove organic contaminants then placed under UV light (254 nm) for 20 min, and immersed in a mixture of H_2O:NH_3·H_2O:H_2O_2 (5:1:1) at 75 °C for 30 min (CAUTION! Reacts violently with organic material. Prepare, handle and dispose of small quantities only). After rinsing with Milli-Q water the sensors were immersed in a solution of $CH_3(CH_2)_{17}SH$ (1 mmol/L in *n*-hexane) for 20 h, rinsed with *n*-hexane, and finally dried under a gentle flow of N_2 gas.

QCM-D Experiments. The lipid film was obtained by dropping and slowly evaporating tristearin solution (10 μL 1 g/L) in chloroform and hexane (1:9) on the thiol-coated QCM-D sensors, causing a frequency decrease of around 1500 Hz. The lipid-coated sensors were then exposed to pure water and QCM-D recording begun when a flat and stable baseline was obtained. After a few minutes the solution was changed to the nanodiamond suspension, depositing nanoparticles on the lipid layer. The buffer was then switched to surfactant solution when the adsorption of nanoparticles reached saturation. Finally, the surfactant solution was changed back to pure water to clean the QCM-D system. Key experiments were carried out in at least duplicate with

mean and standard deviations displayed as error bars in Table 1 and Figures 3 and 4.

RESULTS AND DISCUSSION

Nanodiamond and Colloid Characterization. Transmission electron microscopy imaging of commercial nanodiamond powder of 97% purity (ND97) revealed aggregates several hundred nanometres across with primary particle size 5−6 nm (see the Supporting Information, Figure S1), consistent with the mean size calculated from X-ray powder diffraction using the Scherrer eq (4 nm, see the Supporting Information, Figure S2). The primary particles were seen to be encapsulated in amorphous carbon, lighter in contrast than crystallized regions (see the Supporting Information, Figure S4), with a broad peak at 1600 cm^{-1} in the Raman spectrum ((see the Supporting Information, Figure S2), confirming the presence of what is generally referred to as "sp^2 carbon".[30]

The zeta potential of ND97 was measured in water (pH 7.0 to 7.2) to be ca. 15 mV, consistent with observed poor colloidal stability. A system with zeta potential outside +30 to −30 mV is usually considered stable,[42] and ionic surfactants such as SDBS, SDS and CTAB were found to impart high magnitude zeta potential, even at low concentration (see the Supporting Information, Figures S7 and S8). Nonetheless, zeta potential alone does not estimate colloid stability well, especially in solutions of high ionic strength, since many factors contribute.[42] Hence, we also measured average particle size over time to confirm the stability of nanodiamond suspensions (see the Supporting Information, Figure S9), implying that commercial ND97 is most stable in 2 mmol/L hexadecyltrimethylammonium bromide (CTAB) solution, then 10 mmol/L sodium dodecylbenzenesulfonate (SDBS) solution. Obvious aggregation was seen for ND97 in 40 mmol/L SDBS solution, since the average size of particles kept increasing over a 14-h period, despite a zeta potential of −50 mV.

The adsorption of nonionic or zwitterionic surfactants onto particles will reduce the charge perceived at the shear plane,[42] but the nanoparticles remain stabilized due to the surfactants' kosmotropicity.[43,44] For example, ND97 was found to be very stable in 8 g/L polyethylene glycol (M_n = 1000, PEG-1000) aqueous solution, and reasonably stable in 8 g/L polyethylene glycol dodecyl ether (Brij35) solution ((see the Supporting Information, Figure S10), principally due to the energy required to dehydrate the hydrophilic PEG as any two nanodiamond-surfactant assemblies approach. Interestingly, low stability was seen in a solution of zwitterionic surfactant *N*,*N*-dimethyldodecylamine *N*-oxide (DDAO) above its critical micellar concentration, possibly due to the relatively small, albeit potent hydrophilic moiety in DDAO compared to PEG-1000, or that amphiphile's preference to exist as small micellar assemblies.

In the absence of surfactant, nanodiamond particles did not remove tristearin from surfaces, rather they were adsorbed[45] on a lipid-coated QCM sensor exposed to a suspension of ND97 in water (Figure 1, region (ii)). However, when this nanodiamond-coated surface was exposed to SDBS, the removal of tristearin was significantly enhanced relative to SDBS alone. To quantify this effect we report two frequency changes (a directly observed quantity, rather than mass change, a derived quantity) for each surface treatment, where R_1 represents the baseline−to−equilibrium desorption of surface bound materials including lipid and R_2 the maximum deflection[11] (as previously reported), presenting an average of

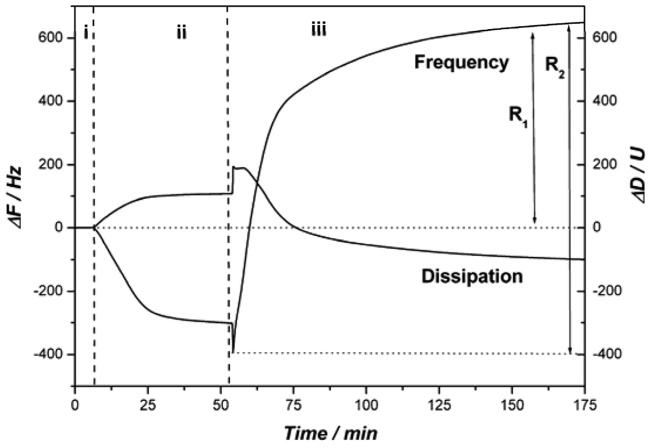

Figure 1. Frequency and dissipation changes to third overtone measured by QCM-D after exposure of the tristearin coated sensor to: region (i) 0−7 min, water; region (ii) 7−52 min, ND97 suspension; region (iii) 52−175 min, SDBS solution. [ND97] = 0.1 g/L, [SDBS] = 40 mmol/L, T = 25 °C; R_1 = 654 Hz, R_2 = 1054 Hz.

two side-by-side experiments with standard deviation (Table 1). Data for individual runs are shown in Figure 2 indicating in this case that ND97-SDBS colloid gives a 23% improvement over SDBS solution (40 mM) alone.

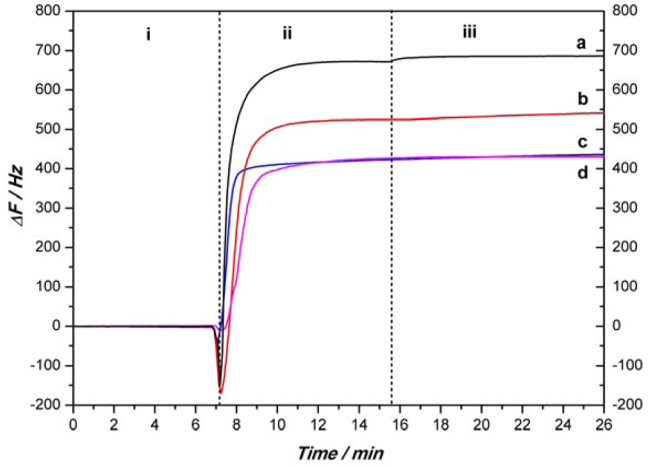

Figure 2. Frequency change to third overtone measured by QCM-D when the tristearin coated sensor is exposed to: region (i) 0−7 min, water is used for both sensors to obtain a stable baseline; region (ii) 7−17 min, (a) G_1C_{10}/ND97 colloid R_1 = 690 Hz, R_2 = 740 Hz, (b) SDBS/ND97 colloid, R_1 = 540, R_2 = 730 Hz, (c) SDBS solution, R_1 = 440, R_2 = 490 Hz, and (d) G_1C_{10} solution R_1 = 440 Hz, R_2 = 440 Hz were used to remove tristearin lipid; region (iii) 17−26 min, SDBS solution was used for sensors b and c, whereas G_1C_{10} solution was used for sensors a and d to clean the QCM system. [SDBS] = 40 mmol/L, [G_1C_{10}] = 3.1 mmol/L, [ND97] = 0.1 g/L, T = 25 °C.

The nonionic surfactants decyl β-D-glucopyranoside (G_1C_{10}) and decyl β-D-maltopyranoside (G_2C_{10}) have been reported[11,17] as effective at removing tristearin at 50 °C,[16] but we observed them to be less so at room temperature. Surfactant G_1C_{10} was still found to remove lipid (Figure 2, R_1 = 440 Hz), increasing to R_1 = 690 Hz in the presence of G_1C_{10}/ND97 colloid, an enhancement of 57%. In contrast, G_2C_{10} was ineffective at room temperature (Figure 3 and the Supporting Information).

If, as has been done previously,[46,47] we assume the Sauerbrey equation applies here, the removal of tristearin by G_1C_{10} in the

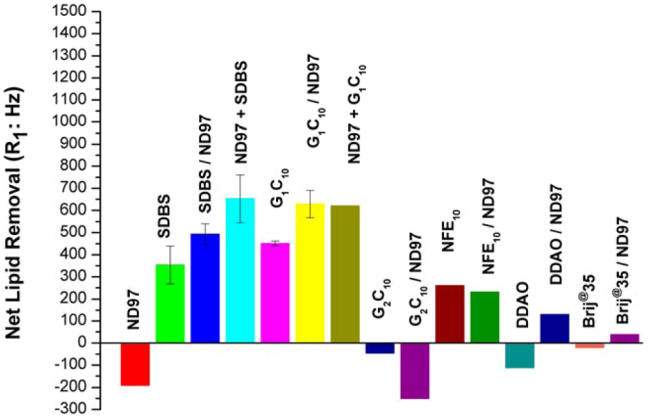

Figure 3. Summary of lipid removal (R_1) obtained by surfactants in the presence or absence of ND97 at 25 °C. SDBS/ND97 represents the colloid of ND97 stabilized by SDBS. ND97+SDBS represents exposure to ND97 suspension in water, followed by SDBS solution. [SDBS] = [DDAO] = 40 mmol/L, [G_1C_{10}] = 3.1 mmol/L, [Brij35] = 8 g/L, [NFE_{10}] = 1.5 wt %, [ND97] = 0.1 g/L, [G_2C_{10}] = 2.1 mmol/L. Error bars represent standard deviation of duplicate measurements.

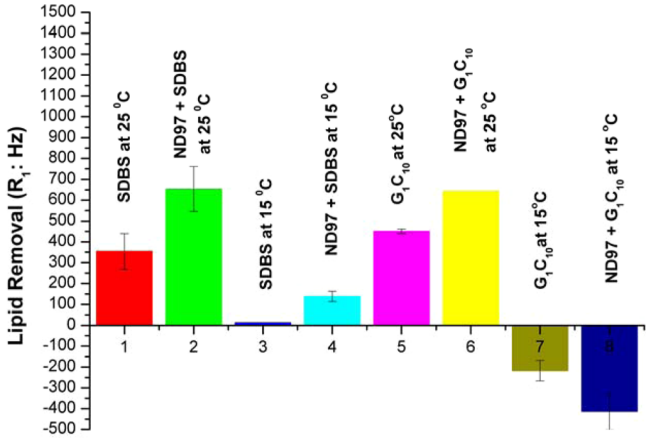

Figure 4. Summary of lipid removal (R_1) obtained by surfactants SDBS or G_1C_{10} in the presence of ND97 at 25 and 15 °C. [SDBS] = 40 mmol/L, [G_1C_{10}] = 3.1 mmol/L, [ND97] = 0.1 g/L. Error bars represent the standard deviation of duplicate measurements.

presence of ND97 can be estimated to be 43%, since evaporating a solution of tristearin (10 μL, 1 g/L) in a mixture of $CHCl_3$ and n-C_6H_{14} (1: 9) on the sensor resulted in around a 1500 Hz decrease in frequency. The observed changes in dissipation also confirmed the removal of lipid from the surface (see the Supporting Information). The improvements in detergency induced by ND97 particles were also seen in the presence of nonionic surfactants Brij35, and for zwitterionic surfactant DDAO, albeit to a much lesser extent (Figure 3). The efficiency of nonionic surfactant NFE_{10} at tristearin removal was not improved in the presence of ND97, although the detergency process proceeded more rapidly (see the Supporting Information, Figures S21–23).

About the same amount of lipid removal was observed for ND97/SDBS, or ND97/G_1C_{10} colloids compared with exposure to ND97 suspension in water followed by surfactant solution (SDBS or G_1C_{10}). Hence interfacial nanodiamond is confirmed as the key player in lipid removal.

This nanodiamond effect is even more significant at lower temperature (Figure 4). As expected, very limited lipid removal (12 Hz) was observed for 40 mmol/L SDBS solution at 15 °C. Dramatic improvement to a value of 161 Hz was seen at the same temperature in the presence of ND97. Nonionic surfactant G_1C_{10} was ineffective at lipid removal when the temperature was decreased to 15 °C, even in the presence of ND97 (see Figure 4 and the Supporting Information).

Nanoparticle Enhanced Cleaning Mechanisms. Nanodiamond has a known ability to adsorb small molecules,[25,26,32] although that alone cannot explain our observations, because nanodiamond by itself is ineffective at removing tristearin from a surface. The beneficial effect of adding a hydrophobic surface to nonionic surfactants[1,20] may be significant in bringing about the observed effects and this could be further tested by measuring the phase inversion temperature of surfactant–lipid mixtures in the presence and absence of nanodiamond or other nanoparticulates. Roughening of an otherwise relatively hydrophobic surface by deposition of the nanoscale objects, effectively lowering the interfacial energy and ability of surfactant to penetrate the lipid–water interface is a third way in which cleaning might be assisted. Finally, the acidic sites or other impurities on the nanodiamond surface could serve to catalyze tristearin hydrolysis, introducing fatty acids that are know to dramatically enhance solubilization rates of triacyl glycerol esters.[48] Any of these mechanisms might be susceptible to alteration in nanodiamond surface chemistry or electrostatic charge. To further investigate these effects and how they might modulate classic mechanisms for removal of lipid from surfaces,[6] we prepared functionalized nanodiamonds by oxidative, reductive, and subsequent photochemical routes (Scheme 1).

Scheme 1. Preparation of Derivatized Diamond Nanoparticles 1–4 from Commercial Nanodiamond Powder (97% purity, Nd97). Reagents and conditions: (i) 485 °C, air, 1-5 h; (ii) H_2 plasma, 10 min; (iii) 10-undecenoic acid, PhMe (or Et_3N), $h\upsilon$, λ = 254 nm, or 1-(4-methylpiperazin-1-yl)undec-10-en-1-one, PhMe, $h\upsilon$, λ = 254 nm

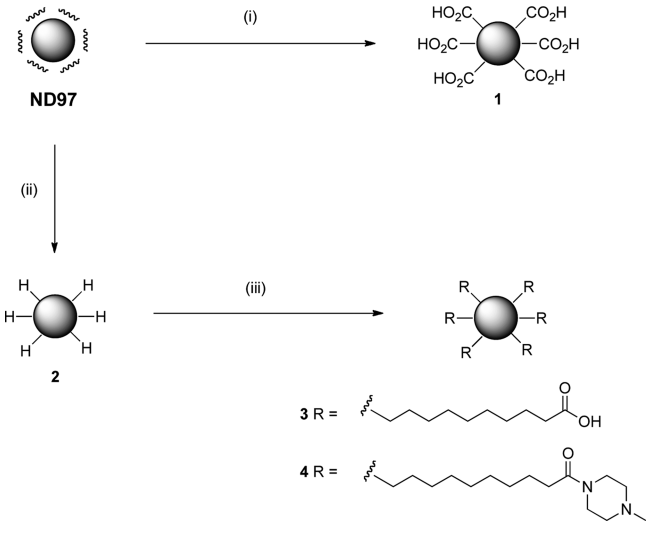

Modification of Nanodiamond. Thermal oxidation is an efficient way to remove some of the 'sp^2' surface carbon, to give polar or ionizable functional groups including carboxylic acids.[30] After heating the nanodiamond powder in air at 400–500 °C to give oxidized product (**1**), Raman spectroscopy and transmission electron microscopy (TEM) (see the

Supporting Information, Figures S3 and S4) clearly revealed that so-called 'sp^2' or amorphous carbon had been selectively removed, with the intensity of the peak at 1330 cm^{-1} relative to that at 1600 cm^{-1} increasing with time of treatment. Infrared spectra revealed a new peak at 1800 cm^{-1} (see the Supporting Information, Figure S11), some 40 cm^{-1} higher than that of carboxyl groups reported previously.[29,30]

To more fully understand this peak, oxidized nanodiamond sample was immersed in aqueous 3 M KOH, whereupon IR spectroscopy of the dried sample showed that the peak had moved to longer wavelength, 1775 cm^{-1}. Upon treatment with aqueous 3 M HCl the absorption returned to 1800 cm^{-1}, indicative of reprotonation of a carboxylate, rather than hydrolysis of a putative anhydride. The reason for the higher wavenumber observed herein for the carboxyl absorbance remains uncertain, but the vibration frequency of surface carbonyls on nanodiamond has been reported to be very sensitive to their local environment, as well as temperature.[49]

Reduction of powder ND97 with hydrogen plasma at an optimized 900 W was used to prepare H-derivatized nanodiamond (**2**). Infrared spectroscopy (see the Supporting Information, Figure S5) confirmed new hydrocarbon bonds on the surface of the particles with peaks at 1394, 1331, and 840 cm^{-1} characterized as alkyl C−H bending with those at 2877 and 2940 cm^{-1} attributed to alkyl C−H stretching. TEM revealed regions of high crystallinity as expected (Figure 5),

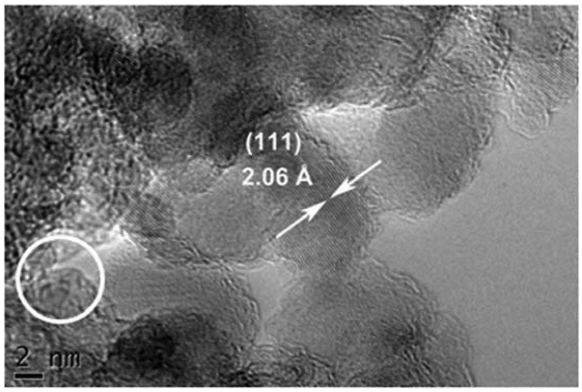

Figure 5. TEM image of **2** obtained from ND97 by hydrogen plasma treatment. Circled area indicates amorphous carbon.

together with areas of amorphous carbon. This reduced material was used as a versatile platform from which to prepare nanodiamond bearing alkyl ω-carboxyl and ω-amine functionality (**3** and **4**, respectively; Scheme 1), through a straightforward photoinitiated reaction.[50−52] Characteristic alkyl chain C−H stretching vibrations at 2852 and 2933 cm^{-1} and other diagnostic peaks such as a new amide carbonyl C═O stretch at 1725 cm^{-1} and N−H bending at 1566 cm^{-1} confirmed the expected functionality. Solid-state CP MAS NMR spectra (Figure 6) demonstrated disappearance of the alkene signals and other features consistent with the expected photoinitiated reaction. Alkyl carbons resonating at 45, 33, and 30 ppm,[53−61] are seen, but no peaks for alkene carbons are observed between 110 and 150 ppm. The signal of carbonyl group at 177 ppm is clearly seen for amido-amine **4** but is weaker in the case of ω-acid **3**, possibly because of difference in dynamics.

These features alone cannot be considered unambiguous proof of covalent attachment, but thermogravimetric analysis

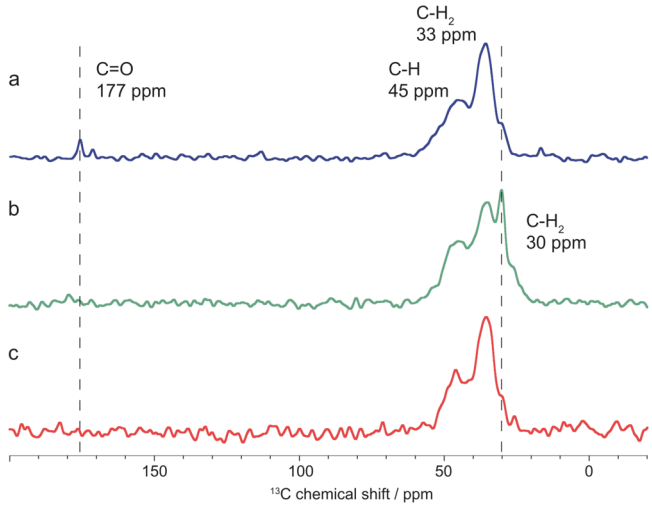

Figure 6. ^{13}C NMR CP MAS spectra of diamond nanoparticles samples (^{1}H Larmor frequency 600 MHz, 20 kHz MAS): (a) alkylamine functionalized diamond nanoparticles **4**; (b) alkylcarboxyl functionalized diamond nanoparticles **3**, and (c) reference spectrum of starting materials **2**.

(see the Supporting Information, Figure S13) additionally showed that there was a clear weight loss at temperatures of up to 250 and 300 °C for sample **4** and sample **3** respectively, confirming that the alkyl chains are in fact covalently attached to the particles. By comparison, only a slight decrease in mass for the starting material **2** was evident below 100 °C, consistent with the loss of surface associated solvent or water, with no other signal visible up to 700 °C.

The zeta potential of commercial nanodiamond ND97 (15 mV) increased to 41.5 mV after treatment with H_2 plasma. Reduction in zeta potential from 41.5 to 26.1 mV was observed after the photoinitiated reaction with ω-alkenylcarboxylate -$(CH_2)_{10}$-COOH, whereas a slight increase to a zeta potential of 48.1 mV was seen after reaction with 1-(4-methylpiperazin-1-yl)undec-10-en-1-one. In contrast, the oxidized nanodiamond samples **1** have a negative zeta potential, of up to −46.5 mV, offering further evidence of carboxylate surface functionality in that material. The zeta potential of oxidized samples also correlates positively with the intensity of carbonyl functional group infrared stretch (Figure 7).

Average aggregate size as a function of time indicated the stability of nanodiamond suspensions (see the Supporting Information, Figure S12), showing that the order is: **1** > **4** > ND97 ≈ **3** > **2** and that neither **2** or **3** are very stable in water, exhibiting aggregation and sedimentation. The oxidized powder **1** was found to be extremely stable with a small aggregate size in water, plausibly because of their negatively charged and hydrophilic surface.

Results for lipid removal by SDBS in the presence of nanodiamonds exhibiting different zeta potentials clearly showed a trend that time to reach equilibrium t increases with the zeta potential of particles (Table 1). For example, in the presence of ND97 with a zeta potential of 15 mV, it took around 120 min to achieve maximum removal, compared to more than 600 min in the presence of amine functionalized nanoparticles **4**, with a zeta potential of 48.1 mV (Figure 8, left). Thus the rate of lipid removal with anionic surfactant SDBS in the presence of nanoparticles follows the order: ND97 > **3** > **2** > **4**, proportional to the strength of electrostatic

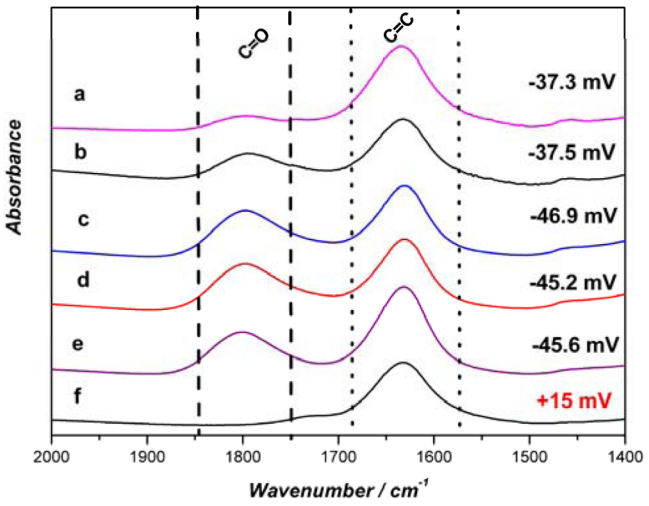

Figure 7. IR spectra with aqueous zeta potential of samples obtained from ND97 by thermal treatment in air as follows: (a) at 495 °C for 3 h; (b) at 485 °C for 5 h; (c) at 485 °C for 3 h; (d) at 485 °C for 1 h; (e) at 425 °C for 5 h; and (f) reference spectrum of ND97. There is a strong correlation between zeta potential and the intensity of the carbonyl stretch.

interactions between anionic surfactant and cationic particles. Furthermore, the presence of a phenyl ring in SDBS, also seen in polyoxoethylene(100) nonylphenyl ether, known to be beneficial in solubilizing carbon nanotubes,[62] may provide additional π-surface interactions that aid both the observed nanodiamond assemblies and lipid removal.

Role of Nanodiamond Particles. Unlike oily soils, solid and crystalline lipids are reported to be removed by direct solubilization, rather than emulsification, or other mechanisms.[6] When surfactant is adsorbed to the lipid surface, repulsive interactions between hydrated, and especially charged headgroups relative to micellar nanodiamond assemblies in suspension provide an energetic driving force for this lipid solubilization process. Introduction of oleic acid to triolein is known to cause rapid and large increase in solubilization rates,[48] and the nanodiamond assemblies might similarly introduce negatively charged headgroups by multiple mechanisms. Headgroup repulsion (whether charge or hydration induced) would be exacerbated at sites of negative curvature where the nanodiamond aggregates meet the lipid interface and hence the roughening of the surface provided by the 5 nm nanodiamonds also seems a key driver in the enhanced lipid removal process (Scheme 2).

The solubilization process is thus directly linked to the presence and size of the particles and would act to enhance the recognized close packing of surfactant molecules on a lipid surface that decreases the energy required for lipid removal.[3,63] This seems a plausible way of aiding a phase inversion process (interfacial water-in-oil to bulk oil-in-water) at the lower temperature observed, although not one that has been described previously. From the present data we cannot distinguish whether the nanodiamonds substantially remain on the surface (Scheme 2c), or are removed along with the lipid-surfactant aggregates (Scheme 2d).

To further investigate the effect of interfacial charge on lipid removal, we exposed tristearin lipid-coated QCM sensors to positively charged diamond nanoparticle suspensions (**2** or **4**, 0.1 g/L), and then **1** colloid (0.1 g/L) followed by SDBS surfactant (40 mmol/L). The negatively charged particles **1** were expected to neutralize the positive zeta potential of the initially deposited particles (**2** or **4**), and weaken the electrostatic attractions between the surfactant and nanoparticles. A colloidal suspension of nanodiamond **1** was successfully deposited on the lipid layer with nanoparticles **4**, reflected by a decrease in frequency after exposure to **1** (Figure 8, right). As expected, there was an initial adsorption after swapping the buffer from **1** to 40 mmol/L SDBS immediately followed by desorption of lipid. However, compared to the lipid removal shown in Table 1, the removal process was now observed to be quicker in the presence of **4** and **1** combined, with a significant decrease in time t from 600 to 200 min. Similar effects were seen for particles **2** (Table 1). These phenomena further confirmed that the rate of lipid removal is largely determined by the interactions between particles and surfactant molecules.[64] They also imply that it is possible to control the removal process by tuning the charge environment on the particle surface.

CONCLUSIONS

Nanodiamond and nanodiamond−surfactant aggregates have been demonstrated for the first time to enhance the removal of tristearin, a model lipid, in the presence of both anionic and

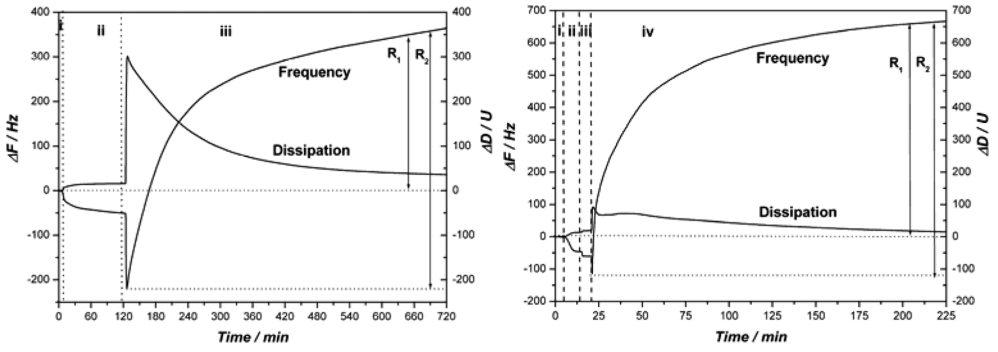

Figure 8. Frequency and dissipation changes to thirrd overtone of the tristearin-coated sensors measured by QCM-D. Left: region (i) 0−7 min, water; region (ii) 7−120 min, amine-functionalized nanodiamond particles **4**; region (iii) 120−720 min, SDBS solution. In the presence of nanoparticles **4** with zeta potential of 48.1 mV, R_1 = 364 Hz, R_2 = 583 Hz in 600 min. Right: region (i) 0−7 min, water; region (ii) 7−14 min, nanodiamond suspension **4**; region (iii) 14−21 min, colloid **1** was used to neutralize the positive charged surface of nanoparticles, and region (iv) 21−225 min, SDBS was used for lipid removal. In the presence of oppositely charge nanoparticles, R_1 = 670 Hz, R_2 = 785 Hz after exposure to SDBS solution for 204 min. Note that equilibrium has not been fully reached in either case; [**4**] =[**1**] = 0.1 g/L, [SDBS] = 40 mmol/L, T = 25 °C.

dx.doi.org/10.1021/am300560z | ACS Appl. Mater. Interfaces 2012, 4, 3225−3232

Scheme 2. Nanodiamond Plays a Key Role in Surfactant-Mediated Removal of Lipid. (a) Adsorption of Nanodiamond–Surfactant Complex May Promote Insertion of Surfactant in Lipid Layer, Interfacial Phase Inversion and Tristearin Lift-off, (b) Lipid–Surfactant Vesicle Budding, (c, d) Solubilization with or without Removal of Nanodiamond from the Surface

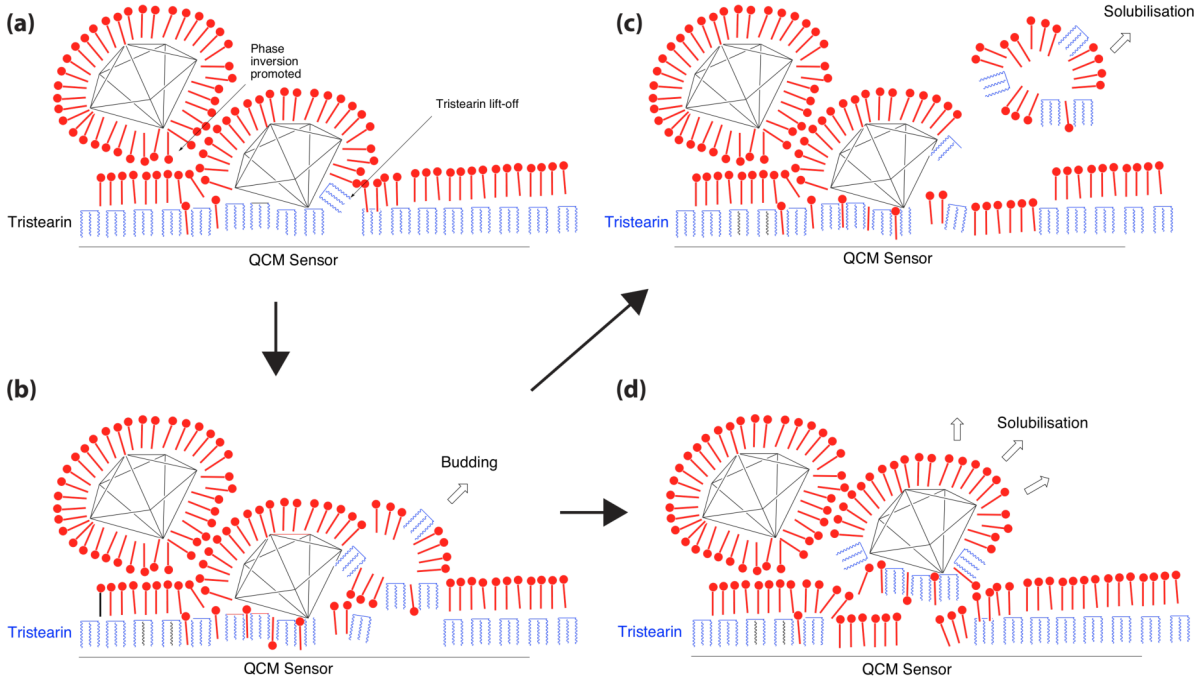

nonionic surfactant. Most significantly, this effect is observed between 15 and 25 °C and the surfactants used are found in typical laundry detergent preparations. Acute, long-term toxicity and other health effects of nanoparticulates are under scrutiny however.[65,66] Together with other commercial and environmental considerations, this may limit their use for this new application at this time. Nanoparticles appear to promote lipid removal by roughening the surface to enhance surfactant adsorption from solution and providing sites of negative curvature at the interface that we suggest serve to lower the energy of phase inversion and perhaps formation of an intermediate phase.[48,67] There is also dependence on nanodiamond surface functionality whereby strong electrostatic interactions between nanoparticles and surfactant encourage adsorption, but hinder the subsequent release of lipid-surfactant aggregates into the solution phase. Lipid removal thus correlates with nanodiamond surface chemistry and zeta potential, providing new tools with which to explore alternative structures that bring similar advantage to this important process.

■ ASSOCIATED CONTENT

Supporting Information

Structures of surfactants and lipid tristearin used. Detailed methods and images for TEM and XRD pattern analysis of untreated nanodiamond powder ND97; curves of the Z-average size of ND97 particles in nonionic surfactant solution, zeta potential of ND97 particles in nonionic solutions, Methods for QCM-D, and QCM-D data for adsorption of nanodiamond suspensions and colloids on tristearin surfaces, including frequency and dissipation changes for lipid removal by SDBS with different concentrations and at different temperatures (15 and 25 °C). Lipid removal by 40 mmol/L SDBS solution in the presence of nanoparticles with different zeta potential, lipid removal by nonionic surfactant G_1C_{10} (3.1 mmol/L and cationic surfactants (2 mmol/L) in the presence or absence of nanoparticles, lipid removal by other surfactants in the presence or absence of nanoparticles. This information is available free of charge via the Internet at http://pubs.acs.org/.

■ AUTHOR INFORMATION

Corresponding Author

*E-mail: a.marsh@warwick.ac.uk.

Notes

The authors declare no competing financial interest.

■ ACKNOWLEDGMENTS

We are grateful to EPSRC and P&G plc for funding (Grant Reference EP/H034269/1) and thank Drs David York and Alan Brooker (P&G plc) for helpful discussions. We thank Dr Richard Walton, Department of Chemistry, University of Warwick for assistance in collecting and analyzing the X-ray powder diffraction patterns, Mr Steve York, Department of Physics, for obtaining the TEM images and Mr Su Shi, School of Engineering and Applied Science, Aston University, for his assistance in CVD treatment of nanodiamond powder and Miss Dorota A. Dobrzanska for the preparation of 1-(4-methyl-4-oxopiperazin-1-yl)undec-10-en-1-one. The QCM-D, powder X-ray diffraction, Raman microscope and light scattering equipment used in this research were obtained through Birmingham Science City: Innovative Uses for Advanced Materials in the Modern World with support from Advantage West Midlands (AWM) and part funded by the European Regional Development Fund (ERDF). EPSRC are thanked for funding solid-state NMR infrastructure and for CASE PhD funding with GlaxoSmithKline for AST.

■ REFERENCES

(1) Raney, K. H.; Benton, W. J.; Miller, C. A. *J. Colloid Interface Sci.* **1987**, *117*, 282.

(2) Raney, K. H.; Miller, C. A. *J. Colloid Interface Sci.* **1987**, *119*, 539.
(3) Backstrom, K.; Lindman, B.; Engstrom, S. *Langmuir* **1988**, *4*, 872.
(4) Sonesson, A. W.; Callisen, T. H.; Elofsson, U. M.; Brismar, H. *J. Surfactants Deterg.* **2007**, *10*, 211.
(5) Thirunavukarasu, K.; Edwinoliver, N. G.; Anbarasan, S. D.; Gowthaman, M. K.; Iefuji, H.; Kamini, N. R. *Process Biochem.* **2008**, *43*, 701.
(6) Miller, C. A.; Raney, K. H. *Colloid Surf., A* **1993**, *74*, 169.
(7) Market Transformation Programme Briefing Note BNW05; DEFRA, Ed. 2008.
(8) Aehle, W. *Enzymes in Industry: production and applications*, 3rd ed.; Wiley-VCH: Weinheim, Germany, 2007.
(9) Snabe, T.; Petersen, S. B. *Chem. Phys. Lipids* **2003**, *125*, 69.
(10) Mori, F.; Lim, J. C.; Raney, O. G.; Elsik, C. M.; Miller, C. A. *Colloids Surf.* **1989**, *40*, 323.
(11) Weerawardena, A.; Drummond, C. J.; Caruso, F.; McCormick, M. *Langmuir* **1998**, *14*, 575.
(12) Robb, I. D.; Stevenson, P. S. *Langmuir* **2000**, *16*, 7939.
(13) Wells, D.; Fong, C.; Krodkiewska, F.; Drummond, C. J. *J. Phys. Chem. B* **2006**, *110*, 5112.
(14) Sonesson, A. W.; Brismar, H.; Callisen, T. H.; Elofsson, U. M. *Langmuir* **2007**, *23*, 2706.
(15) Weerawardena, A.; Drummond, C. J.; Caruso, F.; McCormick, M. *Colloid Surf., A* **1999**, *146*, 185.
(16) Hussain, Y.; Krim, J.; Grant, C. *Colloid Surf., A* **2005**, *262*, 81.
(17) Boyd, B. J.; Drummond, C. J.; Krodkiewska, I.; Weerawardena, A.; Furlong, D. N.; Grieser, F. *Langmuir* **2001**, *17*, 6100.
(18) Rojas, O. J.; Stubenrauch, C.; Schulze-Schlarmann, J.; Claesson, P. M. *Langmuir* **2005**, *21*, 11836.
(19) Tongcumpou, C.; Acosta, E. J.; Quencer, L. B.; Joseph, A. F.; Scamehorn, J. F.; Sabatini, D. A.; Chavadej, S.; Yanumet, N. *J. Surfactants Deterg.* **2003**, *6*, 205.
(20) Beaudoin, S. P.; Grant, C. S.; Carbonell, R. G. *Ind. Eng. Chem. Res.* **1995**, *34*, 3307.
(21) Nickel, D.; vonRybinski, W.; Kutschmann, E. M.; Stubenrauch, C.; Findenegg, G. H. *Fett-Lipid* **1996**, *98*, 363.
(22) Tanthakit, P.; Nakrachata-Amorn, A.; Scamehorn, J.; Sabatini, D.; Tongcumpou, C.; Chavadej, S. *J. Surfactants Deterg.* **2009**, *12*, 173.
(23) Mochalin, V. N.; Shenderova, O.; Ho, D.; Gogotsi, Y. *Nat. Nanotechnol.* **2012**, *7*, 11.
(24) Krueger, A.; Lang, D. *Adv. Funct. Mater.* **2012**, *22*, 890.
(25) Huang, H.; Pierstorff, E.; Osawa, E.; Ho, D. *Nano Lett.* **2007**, *7*, 3305.
(26) Puzyr, A. P.; Baron, A. V.; Purtov, K. V.; Bortnikov, E. V.; Skobelev, N. N.; Moginaya, O. A.; Bondar, V. S. *Diam. Relat. Mater.* **2007**, *16*, 2124.
(27) Ferrari, A. C.; Robertson, J. *Philos. Trans. R. Soc., A* **2004**, *362*, 2477.
(28) Premkumar, T.; Mezzenga, R.; Geckeler, K. E. *Small* **2012**, 10.1002/smll.201101786.
(29) Gibson, N.; Shenderova, O.; Luo, T. J. M.; Moseenkov, S.; Bondar, V.; Puzyr, A.; Purtov, K.; Fitzgerald, Z.; Brenner, D. W. *Diam. Relat. Mater.* **2009**, *18*, 620.
(30) Osswald, S.; Yushin, G.; Mochalin, V.; Kucheyev, S. O.; Gogotsi, Y. *J. Am. Chem. Soc.* **2006**, *128*, 11635.
(31) Takimoto, T.; Chano, T.; Shimizu, S.; Okabe, H.; Ito, M.; Morita, M.; Kimura, T.; Inubushi, T.; Komatsu, N. *Chem. Mater.* **2010**, *22*, 3462.
(32) Chen, M.; Pierstorff, E. D.; Lam, R.; Li, S.-Y.; Huang, H.; Osawa, E.; Ho, D. *ACS Nano* **2009**, *3*, 2016−2022.
(33) Liu, R. H.; Kay, B. K.; Jiang, S. Y.; Chen, S. F. *MRS Bull.* **2009**, *34*, 432.
(34) Rouhana, L. L.; Jaber, J. A.; Schlenoff, J. B. *Langmuir* **2007**, *23*, 12799.
(35) Rodahl, M.; Höök, F.; Fredriksson, C.; A. Keller, C.; Krozer, A.; Brzezinski, P.; Voinova, M.; Kasemo, B. *Faraday Discuss.* **1997**, *107*, 229.
(36) Höök, F.; Rodahl, M.; Kasemo, B.; Brzezinski, P. *Proc. Natl. Acad. Sci. U.S.A.* **1998**, *95*, 12271.
(37) Ohlsson, G.; Tigerstrom, A.; Höök, F.; Kasemo, B. *Soft Matter* **2011**, *7*, 10749.
(38) Reviakine, I.; Johannsmann, D.; Richter, R. P. *Anal. Chem.* **2011**, *83*, 8838.
(39) Voinova, M. V.; Rodahl, M.; Jonson, M.; Kasemo, B. *Phys. Scr.* **1999**, *59*, 391.
(40) Metz, G.; Wu, X. L.; Smith, S. O. *J. Magn. Res., Ser. A* **1994**, *110*, 219.
(41) Khitrin, A.; Fung, B. M. *J. Chem. Phys.* **2000**, *112*, 2392.
(42) Rosen, M. J. *Surfactants and Interfacial Phenomena*; Wiley: New York, 2004.
(43) Kane, R. S.; Deschatelets, P.; Whitesides, G. M. *Langmuir* **2003**, *19*, 2388.
(44) de Gennes, P. G. *Adv. Colloid Interface Sci.* **1987**, *27*, 189.
(45) Caruso, F.; Serizawa, T.; Furlong, D. N.; Okahata, Y. *Langmuir* **1995**, *11*, 1546.
(46) Weerawardena, A.; Boyd, B. J.; Drummond, C. J.; Furlong, D. N. *Colloid Surf., A* **2000**, *169*, 317.
(47) Naderi, A.; Claesson, P. M. *Langmuir* **2006**, *22*, 7639.
(48) Chen, B.-H.; Miller, C. A.; Garrett, P. R. *Langmuir* **1998**, *14*, 31.
(49) Chu, C. D.; Perevedentseva, E.; Yeh, V.; Cai, S. J.; Tu, J. S.; Cheng, C. L. *Diam. Relat. Mat.* **2009**, *18*, 76.
(50) Buriak, J. M. *Chem. Commun.* **1999**, 1051.
(51) Sun, Q.-Y.; de Smet, L. C. P. M.; van Lagen, B.; Giesbers, M.; Thune, P. C.; van Engelenburg, J.; de Wolf, F. A.; Zuilhof, H.; Sudholter, E. J. R. *J. Am. Chem. Soc.* **2005**, *127*, 2514.
(52) Steenackers, M.; Lud, S. Q.; Niedermeier, M.; Bruno, P.; Gruen, D. M.; Feulner, P.; Stutzmann, M.; Garrido, J. A.; Jordan, R. *J. Am. Chem. Soc.* **2007**, *129*, 15655.
(53) Donnet, J.-B.; Fousson, E.; Delmotte, L.; Samirant, M.; Baras, C.; Wang, T. K.; Eckhardt, A. *C. R. Acad. Sci., Ser. IIc: Chim.* **2000**, *3*, 831.
(54) Dubois, M.; Guérin, K.; Petit, E.; Batisse, N.; Hamwi, A.; Komatsu, N.; Giraudet, J.; Pirotte, P.; Masin, F. *J. Phys. Chem. C* **2009**, *113*, 10371.
(55) Shames, A. I.; Panich, A. M.; Kempiski, W.; Alexenskii, A. E.; Baidakova, M. V.; Dideikin, A. T.; Osipov, V. Y.; Siklitski, V. I.; Osawa, E.; Ozawa, M.; Vul, A. Y. *J. Phys. Chem. Solids* **2002**, *63*, 1993.
(56) Panich, A. M. *Diam. Relat. Mat.* **2007**, *16*, 2044.
(57) Alam, T. M. *Mater. Chem. Phys.* **2004**, *85*, 310.
(58) Cunningham, G.; Panich, A. M.; Shames, A. I.; Petrov, I.; Shenderova, O. *Diam. Relat. Mat.* **2008**, *17*, 650.
(59) Fang, X.; Mao, J.; Levin, E. M.; Schmidt-Rohr, K. *J. Am. Chem. Soc.* **2009**, *131*, 1426.
(60) Levin, E. M.; Fang, X. W.; Bud'ko, S. L.; Straszheim, W. E.; McCallum, R. W.; Schmidt-Rohr, K. *Phys. Rev. B* **2008**, *77*.
(61) Schmidt-Rohr, K.; Rawal, A.; Fang, X. W. *J. Chem. Phys.* **2007**, *126*.
(62) Lee, Y.; Geckeler, K. E. *Adv. Mater.* **2010**, *22*, 4076.
(63) Malmsten, M.; Lindman, B. *Langmuir* **1989**, *5*, 1105.
(64) Weiss, J.; McClements, D. J. *Langmuir* **2000**, *16*, 5879.
(65) Krueger, A. *J. Mater. Chem.* **2011**, *21*, 12571.
(66) Mohan, N.; Chen, C. S.; Hsieh, H. H.; Wu, Y. C.; Chang, H. C. *Nano Lett.* **2010**, *10*, 3692.
(67) Buchanan, M.; Egelhaaf, S. U.; Cates, M. E. *Langmuir* **2000**, *16*, 3718.